arXiv:2608.09248v2 [cs.AI] 11 Aug 2026

EMOTION2SKILL: Model-Internal Emotion Signals for Adaptive Skill Selection and Evolution

Bohan Lin[1,2], **Hejia Geng**[3], **Xinyi Xie**[4], **Heng Zhou**[1,5], **Qinghua Xing**[1], **Bo Liu**[4], **Chen Zhang**[5,*], **Yudong Zhang**[1,2,*]

[1]University of Science and Technology of China (USTC)
[2]Suzhou Institute for Advanced Research, USTC
[3]University of Oxford [4]University of Arizona [5]Shanghai AI Laboratory
Contact: linbohan@ustc.edu, yudong.zhang@ustc.edu.cn

Abstract

Skill-based LLM agents select reusable procedures from an external library to solve complex tasks, yet their routing decisions rely entirely on text-level signals such as task descriptions, verbal reflections, and experience-derived rules, while the model's own internal representational state remains unobserved. Recent interpretability work has shown that LLMs maintain linear emotion representations that causally influence behavior; however, these representations have been exploited only for post-hoc analysis or direct output steering, and have not been used to inform agent-level decision-making. We propose EMOTION2SKILL, a framework that extracts LLM-internal emotion vectors and incorporates them into both skill selection and skill evolution. At each decision step, a 27-dimensional emotion state is extracted from the residual stream and mapped to a confidence-gated summary injected into the routing prompt. Beyond online selection, emotion trajectories are analyzed for abrupt internal-state shifts to pinpoint problematic skill invocations, guiding targeted SOP rewriting that replaces the coarse binary outcome signal of prior methods. On WebShop and ALFWorld, EMOTION2SKILL with Qwen3-8B improves over the Zero-Shot baseline by **+26.9%** success rate and **+25.5%** average success respectively, outperforming all baselines on both benchmarks with consistent gains on Qwen3-14B. Co-activation analysis further reveals semantically coherent emotion–skill pairings, confirming that the routing improvements reflect meaningful internal-state signals rather than opaque statistical correlations. These results establish LLM-internal emotion representations as an effective decision-level signal for orchestrating agent skill systems, extending their utility beyond interpretability and output steering. The code is available at https://github.com/BoHan-LIN04/Emotion2Skill.

1 Introduction

Skill-based LLM agents solve complex, long-horizon interactive tasks by retrieving reusable procedural knowledge from external libraries (Wang et al. 2024; Yang et al. 2026d; Yu et al. 2026; Ni et al. 2026). While recent work has substantially advanced skill evolution (Yang et al. 2026d; Yu et al. 2026), trajectory distillation (Ni et al. 2026), and unified skill training (Shi et al. 2026), the quality of skill *selection* continues to bound overall task performance. No amount of skill refinement compensates for systematically retrieving an inappropriate procedure at decision time. Effective skill selection requires conditioning on two complementary sources of information. The first is the *external textual context*: the task description, conversation history, and environment observations that standard agents already exploit. The second is the model's own *internal state*: its accumulated uncertainty, its assessment of prior action outcomes, and the trajectory-level confidence it has built up to the current step. Identical external contexts can demand different skills depending on this internal state, yet no existing skill-selection method directly observes or leverages it.

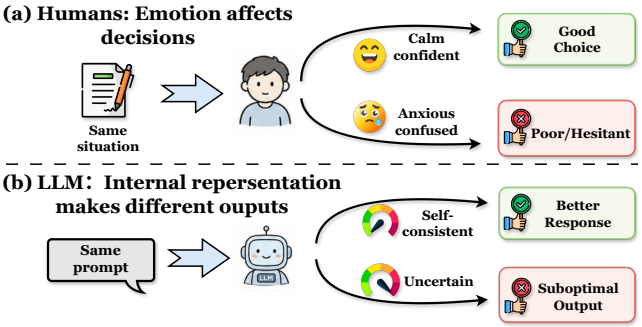

Figure 1: Human decision-making integrates external stimuli with internal affective states. We ask whether LLM agents can exploit an analogous signal: the emotion representations encoded in the model's own residual stream, extracted at inference time and used to condition skill utilization.

Existing approaches to skill selection rely primarily on explicit textual artifacts. Text-embedding retrieval (Wang et al. 2024; Yu et al. 2026) matches task descriptions against skill descriptions in a shared semantic space, verbal self-reflection (Shinn et al. 2023) produces textual critiques of prior actions to inform subsequent choices, experience-based learning (Zhao et al. 2024) distills trajectory-level lessons into natural-language rules, and model-aware alignment (Yu et al. 2026) refines skill content through text-space search. Although effective and complementary, these methods share a structural limitation, namely that they operate exclusively on the external textual context while the model's internal representational state at the moment of selection remains unobserved. The latent component of the selection problem

*Chen Zhang and Yudong Zhang are the corresponding authors.

is therefore systematically absent from the routing decision.

Neuroscience and psychology have long established that human decisions are shaped not only by external stimuli but also by internal affective states (Damasio 1994; Lerner et al. 2015) (Figure 1). We ask whether an analogous principle holds for LLMs. Recent interpretability work shows that LLMs encode linear, causal emotion representations in their residual streams (Zou et al. 2023; Sofroniew et al. 2026) that can be read out at inference time and that *causally* influence agentically relevant outputs such as reward-hacking and sycophancy rates (Sofroniew et al. 2026). Unlike generic hidden-state features, emotion vectors are causally linked to model behavior, interpretable by construction (each dimension names a specific affect), and task-independent, making them a natural proxy for the agent's internal decision state. **Skill selection should therefore incorporate the agent's internal decision state alongside external textual context, and emotion vectors offer an interpretable, causal proxy for doing so.**

Building on this insight, we propose EMOTION2SKILL, a framework that augments LLM-based skill selection with an explicit emotion-derived signal. At each decision step, the agent's emotion state is extracted from the model's residual stream and passed through a lightweight encoder that produces a natural-language emotion template together with a confidence score. This emotion summary is concatenated into the LLM's selection prompt as auxiliary context, and a confidence-gating mechanism omits the signal when it is uninformative. Beyond selection, emotion trajectories recorded during episodes are analyzed for abrupt internal state shifts, and the resulting diagnostics guide periodic skill evolution by directing the rewriter's attention to problematic trajectory segments. On WebShop (Yao et al. 2022) and ALFWorld (Shridhar et al. 2021), EMOTION2SKILL with Qwen3-8B (Yang et al. 2025) improves over the Zero-Shot baseline by **+25.5%** average success on ALFWorld and **+26.9%** success rate on WebShop, outperforming all existing baselines with consistent gains on Qwen3-14B.

Our contributions are as follows.

- We reveal the connection between LLM-internal emotion vectors and agent skill selection, showing empirically that emotion representations encode decision-relevant information absent from text-level features.
- We design EMOTION2SKILL, a framework that leverages emotion vectors for both skill selection and skill evolution in LLM-based agents.
- We conduct extensive experiments on two interactive benchmarks against five baselines, together with ablation studies and interpretability analyses that validate the effectiveness of the proposed approach.

2 Related Work

LLM internal representations and emotion vectors. A growing body of work shows that LLM internal representations encode high-level semantic concepts as linear directions in activation space (Zou et al. 2023; Park, Choe, and Veitch 2024; Nanda, Lee, and Wattenberg 2023) that can be read out at inference time (Burns et al. 2023; Li et al. 2023) and causally steered to alter model behavior (Turner et al. 2023; Panickssery et al. 2024). Sofroniew et al. (2026) demonstrate that frontier LLMs maintain fine-grained emotion directions aligned with the 27-category GoEmotions taxonomy (Demszky et al. 2020) that causally influence agentically relevant behaviors; concurrent mechanistic studies further show that such emotion structure non-monotonically shapes agent reasoning and safety (Sun et al. 2026; Shou and Guan 2026). We adopt these categorical directions rather than appraisal vectors (Scherer 2001) or valence-arousal subspaces, as they are the representation for which causal influence on agent behavior has been directly demonstrated, and named affective categories provide interpretable routing rationales without additional grounding. EMOTION2SKILL is the first to use emotion vectors as an active routing and evolution signal for agent skill systems, moving beyond post-hoc analysis and direct output steering.

Skill-based LLM agents. Skill-based LLM agents maintain reusable procedural knowledge for long-horizon tasks (Wang et al. 2024; Yang et al. 2026d; Yu et al. 2026; Ni et al. 2026), with recent work advancing skill evolution (Yang et al. 2026d; Yu et al. 2026; Wang et al. 2025; Yang et al. 2026a), trajectory distillation (Ni et al. 2026), unified training (Shi et al. 2026), and experiential learning (Zhao et al. 2024; Shinn et al. 2023; Xu et al. 2026). Concurrent work advances complementary dimensions of skill learning: ARISE (Li et al. 2026) introduces hierarchical reinforcement learning over intrinsic skill representations; OPID (Yang et al. 2026c) applies on-policy self-distillation for dense skill-level supervision; Skill-R1 (Vishe et al. 2026) and ReSkill (He et al. 2026) evolve skills via outcome-based and RL-in-the-loop objectives; and MAGE (Yang et al. 2026b) co-evolves skill knowledge graphs across multiple agents. These approaches and EMOTION2SKILL operate on different dimensions: where they optimize skill routing through external reward or similarity feedback, EMOTION2SKILL conditions on the model's internal affective state, and the two classes of signal are complementary rather than directly comparable.

3 Method

EMOTION2SKILL grounds skill decisions in the model's own affective representations, filling the gap left by context-only skill routing. **Emotion Vectors** are extracted from the residual stream and projected into a natural-language summary at each step. **Emotion-Augmented Skill Selection** injects this summary into the routing prompt via a confidence gate. **Emotion-Driven Skill Evolution** detects abrupt trajectory shifts to localize and rewrite underperforming skills. Figure 2 illustrates the design.

3.1 Preliminaries

Consider an agent equipped with a skill library $\mathcal{S} = \{s_1, \ldots, s_M\}$, where each skill s_i is a reusable procedure described by a natural-language SOP D_i. At decision step t, the agent observes the external textual context x_t (task instruction, conversation history, and environment observations) and possesses a latent internal decision state encoded in the residual stream of the underlying LLM. We denote by

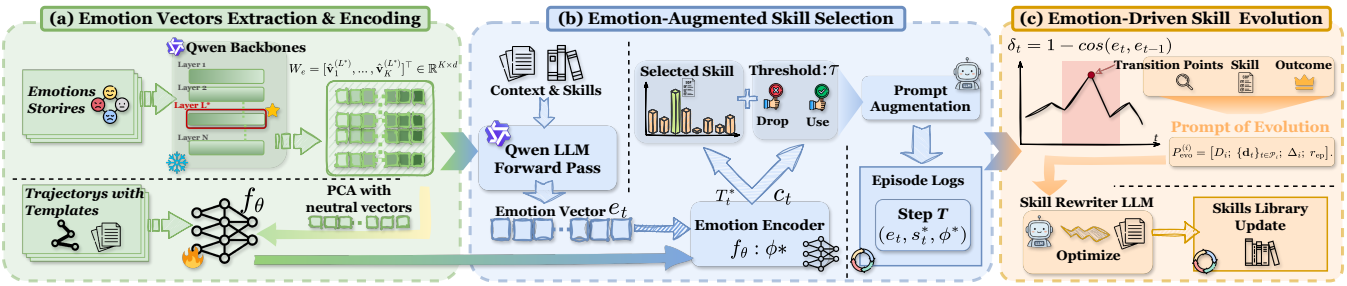

Figure 2: Framework of our method. Left: offline extraction of emotion vectors from the LLM residual stream and MLP encoder training. Middle: emotion state mapped to a confidence-gated summary injected into the skill-selection prompt. Right: emotion trajectory shifts trigger targeted SOP rewriting for underperforming skills.

$\mathbf{h}_t^{(\ell)} \in \mathbb{R}^d$ the residual-stream activation at layer ℓ and token position t, and by L^* the optimal extraction layer selected on validation data.

Standard skill-based agents select a skill s_t^* by prompting the LLM $\mathcal{M}$ with x_t and the candidate SOPs $\{D_1, \ldots, D_M\}$, relying entirely on the textual content of these inputs. EMOTION2SKILL extends this formulation by additionally conditioning on an emotion summary ϕ_t derived from the agent's internal state:

$$s_t^* = \mathcal{M}\big(x_t,\ \{D_1, \ldots, D_M\},\ \phi_t\big), \tag{1}$$

where ϕ_t is a natural-language token sequence produced by a learned emotion encoder f_θ. The LLM remains the primary decision-maker; ϕ_t serves as auxiliary context that makes the agent's latent state explicit.

3.2 Emotion Vector Extraction and Encoding

Contrastive extraction. We extract emotion directions from the agent model following the contrastive-averaging procedure of Sofroniew et al. (2026), replicated on Qwen3. For each of the K=27 emotion concepts in the GoEmotions taxonomy (Demszky et al. 2020), the model generates N=100 short stories with the target emotion. A forward pass through each story yields activations $\mathbf{h}_t^{(\ell)}$ at every layer ℓ and token position t. We mean-pool over tokens past an initial prefix ($t \geq 50$) to obtain a per-story representation $\bar{\mathbf{h}}^{(\ell)}$, then compute the emotion direction for concept k at layer ℓ by subtracting the global mean from the within-concept mean:

$$\mathbf{v}_k^{(\ell)} = \frac{1}{N}\sum_{n=1}^{N} \bar{\mathbf{h}}_{k,n}^{(\ell)} - \frac{1}{KN}\sum_{k'=1}^{K}\sum_{n=1}^{N} \bar{\mathbf{h}}_{k',n}^{(\ell)}. \tag{2}$$

To suppress variance attributable to stylistic rather than affective content, a PCA-based denoising step projects out the top principal components of emotionally neutral activations, yielding denoised directions $\hat{\mathbf{v}}_k^{(\ell)} = \Pi^{\perp}\mathbf{v}_k^{(\ell)}$. The optimal layer L^* is selected from a candidate grid by maximizing GoEmotions classification accuracy . Stacking the denoised directions yields the emotion extractor matrix $W_e = [\hat{\mathbf{v}}_1^{(L^*)}, \ldots, \hat{\mathbf{v}}_K^{(L^*)}]^\top \in \mathbb{R}^{K\times d}$.

At inference time, the raw emotion state at decision step t is obtained by projecting the residual-stream activation at the `Assistant:` delimiter token (Sofroniew et al. 2026) through W_e and applying ℓ_2 normalization:

$$\mathbf{e}_t = \frac{W_e\,\mathbf{h}_T^{(L^*)}}{\|W_e\,\mathbf{h}_T^{(L^*)}\|_2} \in \mathbb{R}^K. \tag{3}$$

The resulting vector $\mathbf{e}_t$ assigns a scalar activation to each of the K emotion dimensions, capturing the agent's affective state at the moment immediately preceding generation.

Emotion encoder. The raw vector $\mathbf{e}_t$ is not directly consumable by the LLM's text-based prompt; naively reporting the top-k activated emotion names as tokens discards magnitude information and ignores interactions between co-activated emotions. We therefore introduce a lightweight *emotion encoder* f_θ that maps $\mathbf{e}_t$ to two outputs used for prompt augmentation. The encoder is a 3-layer MLP that produces an encoded representation $\mathbf{r}_t = f_\theta(\mathbf{e}_t) \in \mathbb{R}^{d'}$. From $\mathbf{r}_t$ we derive (i) a *template index* over a predefined bank $\mathcal{T} = \{T_1, \ldots, T_C\}$ of C=12 natural-language emotion-state descriptions, where each template T_j is associated with a learnable prototype $\mathbf{q}_j \in \mathbb{R}^{d'}$:

$$T_t^* = \arg\max_{T_j \in \mathcal{T}} \frac{\mathbf{r}_t^\top \mathbf{q}_j}{\|\mathbf{r}_t\|\,\|\mathbf{q}_j\|}, \tag{4}$$

and (ii) a scalar *confidence score*

$$c_t = \sigma(\mathbf{w}_c^\top \mathbf{r}_t + b_c) \in [0, 1] \tag{5}$$

indicating how informative the current emotion state is for routing. We define the composite emotion summary as the pair $\phi_t = (T_t^*, c_t)$. When $c_t < \tau$, ϕ_t is omitted from the prompt entirely (confidence gating), allowing the system to fall back to standard text-only selection.

The encoder is trained on tuples $(\mathbf{e}_t, s_t^{\text{sel}}, y_t)$ collected during a warm-up phase in which the agent runs episodes under a baseline policy (ReAct with the skill library, without emotion signals), where $s_t^{\text{sel}} \in \mathcal{S}$ is the baseline's skill choice and $y_t \in \{0, 1\}$ is the episode outcome. The objective combines a supervised-contrastive loss (Khosla et al. 2020) that clusters representations by effective skill assignments with a template-classification loss. For an anchor $\mathbf{r}_i$ with positive set $\mathcal{A}^+(i) = \{j \mid s_j^{\text{sel}}{=}s_i^{\text{sel}} \wedge y_j{=}1\}$, the contrastive term is

$$\mathcal{L}_{\text{ctr}} = -\frac{1}{|\mathcal{B}|}\sum_{i\in\mathcal{B}} \frac{1}{|\mathcal{A}^+(i)|} \sum_{j\in\mathcal{A}^+(i)} \log \frac{\exp(\mathbf{r}_i^\top \mathbf{r}_j/\kappa)}{\sum_{k\neq i}\exp(\mathbf{r}_i^\top \mathbf{r}_k/\kappa)}, \tag{6}$$

where κ is a temperature and representations are ℓ_2-normalized. The classification term assigns pseudo-labels $\hat{c}_t$ via k-means ($k{=}C$) on the raw emotion vectors and minimizes the cross-entropy over prototype similarities:

$$\mathcal{L}_{\text{cls}} = -\frac{1}{|\mathcal{B}|}\sum_{i\in\mathcal{B}} \log \frac{\exp(\mathbf{r}_i^\top \mathbf{q}_{\hat{c}_i}/\kappa')}{\sum_{j=1}^{C}\exp(\mathbf{r}_i^\top \mathbf{q}_j/\kappa')}. \tag{7}$$

The overall objective is $\mathcal{L} = \mathcal{L}_{\text{ctr}} + \lambda\,\mathcal{L}_{\text{cls}}$, where λ balances the two terms.

3.3 Emotion-Augmented Skill Selection

The emotion summary ϕ_t produced by the encoder is concatenated into the LLM's input prompt as additional context, making the agent's latent state visible alongside the task description and candidate skill SOPs. At each decision step t, the system constructs an augmented prompt P_t by appending the emotion template T_t^* and the confidence score c_t to the standard prompt components. When the encoder's confidence falls below the threshold τ, the emotion fields are withheld, and the prompt reduces to the conventional text-only format:

$$P_t = \begin{cases} \big[x_t;\ \{D_i\}_{i=1}^{M};\ T_t^*;\ c_t\big] & \text{if } c_t \geq \tau, \\ \big[x_t;\ \{D_i\}_{i=1}^{M}\big] & \text{otherwise.} \end{cases} \tag{8}$$

The LLM then reads P_t in its entirety and produces a skill decision via constrained generation over the valid skill identifiers:

$$s_t^* = \arg\max_{s_i\in\mathcal{S}}\ p_{\mathcal{M}}(s_i \mid P_t), \tag{9}$$

where $p_{\mathcal{M}}(s_i \mid P_t)$ denotes the conditional probability that $\mathcal{M}$ assigns to skill s_i. The emotion summary enters through the same input channel as the task description, and setting $\tau{=}1$ recovers standard text-only selection.

3.4 Emotion-Driven Skill Evolution

Beyond online selection, the episode log $\mathcal{L}_{\text{ep}}$ provides a temporally ordered trace of internal states that can inform periodic skill evolution. Standard evolution methods (Yang et al. 2026d; Yu et al. 2026) prompt the LLM to rewrite underperforming skill SOPs based on binary episode outcomes and, optionally, textual self-reflection. This signal is coarse in that it arrives only after episode termination and provides no indication of *which* intermediate steps were problematic.

EMOTION2SKILL augments the rewriter's input with structured emotion diagnostics that localize critical state changes within the episode.

Let $\mathcal{E} = (\mathbf{e}_1, \ldots, \mathbf{e}_T)$ denote the emotion trajectory of a completed episode. To identify steps at which the agent's internal state shifted abruptly, we compute the step-to-step *emotion shift magnitude*

$$\delta_t = 1 - \frac{\mathbf{e}_t^\top \mathbf{e}_{t-1}}{\|\mathbf{e}_t\|\ \|\mathbf{e}_{t-1}\|}, \quad t = 2, \ldots, T. \tag{10}$$

This quantity measures the cosine distance between consecutive emotion states and is agnostic to which specific dimensions change; large δ_t indicates a sharp reorganization of the agent's internal state regardless of whether the shift involves positive-valence, negative-valence, or cognitive dimensions. An *emotion transition point* is defined as a step at which δ_t exceeds the episode mean by more than one standard deviation:

$$\mathcal{P} = \big\{t \in \{2, \ldots, T\} \;\big|\; \delta_t > \bar{\delta} + \sigma_\delta\big\}, \tag{11}$$

where $\bar{\delta} = (T{-}1)^{-1}\sum_{t=2}^{T}\delta_t$ and $\sigma_\delta = \big((T{-}1)^{-1}\sum_{t=2}^{T}(\delta_t - \bar{\delta})^2\big)^{1/2}$. By operating on the full K-dimensional emotion vector without pre-selecting specific dimensions, this criterion captures any substantial internal reorganization, including shifts from exploratory states to frustrated states, from confident states to confused states, or from one cognitive mode to another.

For each skill s_i flagged for evolution, we restrict to skill-specific transitions $\mathcal{P}_i = \{t \in \mathcal{P} \mid s_t^* = s_i\}$ and extract a diagnostic context around each:

$$\mathbf{d}_t = (x_{t-1:t+1},\ s^*_{t-1:t+1},\ T^*_{t-1:t+1},\ \delta_{t-1:t+1}), \tag{12}$$

capturing a 3-step window of observations, skill choices, emotion templates, and shift magnitudes. These diagnostics, together with a verbalized summary Δ_i describing the transition pattern, are appended to the evolution prompt alongside the current SOP D_i and the episode outcome r_{ep}:

$$P_{\text{evo}}^{(i)} = \big[D_i;\ \{\mathbf{d}_t\}_{t\in\mathcal{P}_i};\ \Delta_i;\ r_{\text{ep}}\big]. \tag{13}$$

The rewriter receives $P_{\text{evo}}^{(i)}$ as its full input context and generates the revised SOP:

$$D_i' = \mathcal{M}\big(P_{\text{evo}}^{(i)}\big). \tag{14}$$

Evolution proceeds over R rounds; at each round the agent executes a batch of episodes, identifies transition points, and updates each underperforming skill (success rate $< \eta$):

$$\mathcal{S}^{(r+1)} = \big(\mathcal{S}^{(r)} \setminus \{s_i\}\big) \cup \{s_i'\}, \quad \forall\, s_i \in \mathcal{U}^{(r)}, \tag{15}$$

where $\mathcal{U}^{(r)}$ is the set of underperforming skills in round r. The emotion diagnostics enter through the same prompt channel as the SOP and episode transcript, providing temporally localized context that complements the coarse binary outcome signal. Algorithm 1 summarizes both the online selection and the evolution procedure.

4 Experiments

4.1 Setup

We evaluate on **WebShop** (Yao et al. 2022) (web-based shopping; metrics: Score, Succ.%) and **ALFWorld** (Shridhar et al. 2021) (text-based household tasks, 134 test episodes across six task types, `json_2.1.1` split; metric: per-type and average Success%). We compare against Zero-Shot, ReAct (Yao et al. 2023), Reflexion (Shinn et al. 2023), ExpeL (Zhao et al. 2024), and MASA (Yu et al. 2026); all methods are reproduced on both Qwen3-8B and Qwen3-14B (Yang et al. 2025).All experiments are conducted on 8×H800 GPUs.Detailed dataset statistics, baseline reproduction protocols, and hyperparameter configurations are provided in the Technical Supplement.

EMOTION2SKILL uses confidence threshold $\tau{=}0.3$, with the extraction layer L^* selected via GoEmotions classification accuracy . Skill libraries, prompt templates, and further implementation details are provided in Appendix (See supplement materials). Qwen3-14B reuses the same skill libraries and τ; only L^* is re-selected.

Algorithm 1: EMOTION2SKILL

Require: Skill library $\mathcal{S}$, extractor W_e, encoder f_θ, threshold τ, layer L^*, rounds R, threshold η

Online: Emotion Extraction and Skill Selection
for each episode **do**
  $\mathcal{L}_{\text{ep}} \leftarrow \emptyset$
  for each decision step t **do**
    Extract $\mathbf{e}_t \leftarrow W_e\,\mathbf{h}_T^{(L^*)} / \|W_e\,\mathbf{h}_T^{(L^*)}\|_2$; encode $(\mathbf{r}_t, c_t) \leftarrow f_\theta(\mathbf{e}_t)$
    Construct P_t via Eq. 8 (include T_t^*, c_t if $c_t \geq \tau$; omit otherwise)
    $s_t^* \leftarrow \arg\max_{s_i} p_{\mathcal{M}}(s_i \mid P_t)$; execute s_t^*
    Append $(\mathbf{e}_t, c_t, s_t^*, T_t^*)$ to $\mathcal{L}_{\text{ep}}$
  end for
end for

Periodic: Emotion-Augmented Skill Evolution
for round $r = 1, \ldots, R$ **do**
  Compute emotion shifts δ_t (Eq. 10) and transition points $\mathcal{P}$ (Eq. 11) from episode logs
  for each $s_i \in \mathcal{U}^{(r)}$ with success $< \eta$ **do**
    Build $P_{\text{evo}}^{(i)}$ from diagnostics around $\mathcal{P}_i$ (Eqs. 12–13)
    $D_i' \leftarrow \mathcal{M}(P_{\text{evo}}^{(i)})$; $\mathcal{S} \leftarrow (\mathcal{S} \setminus \{s_i\}) \cup \{s_i'\}$
  end for
end for

4.2 Emotion Vector Quality and Layer Selection

We evaluate whether Qwen3-8B's residual stream encodes discriminable emotion structure by benchmarking each candidate layer on the GoEmotions dataset (Demszky et al. 2020) and simultaneously select the optimal extraction layer L^*.

GoEmotions evaluation protocol. We use the GoEmotions test set (27 emotion categories) as the evaluation benchmark. For each candidate layer $\ell \in \{16, 18, 20, 22, 24, 26, 28\}$ (Qwen3-8B, 36 layers), we extract the residual-stream activations at layer ℓ for each GoEmotions example, project onto the emotion directions $\hat{\mathbf{v}}_k^{(\ell)}$ obtained via contrastive averaging, and classify each example by assigning it to the emotion direction with the highest cosine similarity. This evaluation measures how well the emotion directions at each layer recover the human-annotated GoEmotions labels without any task-specific fine-tuning. Because GoEmotions is multi-label, we adopt a *hit-any* criterion: a prediction is correct if the highest-similarity emotion direction matches any of the annotated labels. Under this criterion, a random baseline achieves 8.2% accuracy estimated by uniform sampling over the 27 categories against the empirical multi-label distribution.

Layer selection. Figure 3a reports the 27-class classification accuracy at each candidate layer. Performance does not increase monotonically: accuracy jumps from 15.8% at layer 16 to 24.3% at layer 18, dips to 21.7% at layer 20, then climbs through 30.5% at layer 22 to a peak of $\mathbf{37.2}\%$ at **layer 24**. Subsequent layers show a partial rebound with 35.1% at layer 28 compared with 33.6% at layer 26, indicating that emotion-relevant information does not decay smoothly

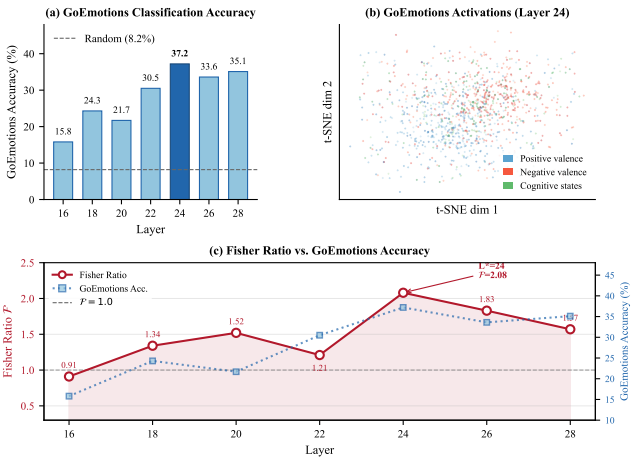

Figure 3: Emotion vector quality and layer selection (Qwen3-8B). (a) GoEmotions 27-class accuracy across layers; non-monotonic profile peaks at layer 24 (37.2%; dashed: random baseline 8.2%). (b) t-SNE of GoEmotions test activations at L^*=24; valence regions are distinguishable but show substantial overlap. (c) Fisher discriminability ratio peaks at layer 24 ($\mathcal{F}$=2.08) but does not track accuracy monotonically.

but redistributes across late layers. The peak at $24/36$=0.67 depth is broadly consistent with Sofroniew et al.'s (2026) observation that emotion representations concentrate near two-thirds depth, though the non-monotonic profile suggests additional layer-specific specialization. We fix L^*=24 for all Qwen3-8B experiments. For Qwen3-14B (40 layers), a separate sweep over $\{18, 20, 22, 24, 26, 28, 30\}$ yields L^*=26 with an accuracy of 39.4%.

Cluster structure. Figure 3b visualizes GoEmotions test activations at layer 24 via t-SNE. Clear valence-level groupings emerge: positive-valence emotions (*joy*, *love*, *optimism*) concentrate in the lower-left quadrant, while negative-valence emotions (*anger*, *disgust*, *sadness*) occupy the upper-right, and cognitive states (*curiosity*, *confusion*) form a distinct intermediate region. Fine-grained categories within the same valence band partially overlap, reflecting the inherent proximity of closely related affects (e.g., *anger* vs. *annoyance*). This structure confirms that the residual stream organizes emotion information along interpretable axes and motivates the use of a learned encoder that can exploit the full 27-dimensional geometry rather than relying on hard low-dimensional cluster assignments.

Fisher discriminability. Fisher's ratio $\mathcal{F}=\sigma^2_{\text{between}}/\sigma^2_{\text{within}}$ peaks at layer 24 with $\mathcal{F}=\mathbf{2.08}$ exceeding 1.0, but does not track accuracy perfectly across layers: at layer 20, $\mathcal{F}$=1.52 alongside a classification accuracy drop to 21.7%, while layer 22 achieves higher accuracy at 30.5% yet presents a lower $\mathcal{F}$=1.21. This partial decoupling suggests that high inter-class separation alone is insufficient: classification accuracy additionally depends on intra-class compactness and the geometry of class boundaries, both of which peak at layer 24.

Backbone	Method	ALFWorld (Success %)							WebShop	
		Pick	Look	Clean	Heat	Cool	Pick2	Avg.	Score	Succ.
Qwen3-8B	Zero-Shot	43.4	39.1	19.1	9.6	12.3	4.4	21.9±1.5	11.2	2.8±0.5
	ReAct (Yao et al. 2023)	53.1	**42.0**	41.3	20.7	18.4	3.6	30.7±1.2	12.1	5.2±3.2
	Reflexion (Shinn et al. 2023)	52.2	34.4	29.0	24.1	19.1	14.1	31.5±1.6	22.4	6.8±2.4
	ExpeL (Zhao et al. 2024)	61.2	30.1	44.4	35.6	28.7	11.5	37.0±4.7	39.6	18.8±4.1
	MASA (Yu et al. 2026)	55.1	24.1	46.6	48.9	43.9	23.4	43.3±0.9	44.7	27.1±0.8
	EMOTION2SKILL (Ours)	**67.9**	37.1	**47.2**	**56.9**	47.2	**31.3**	**47.4**±1.6	**52.1**	**29.7**±1.6
Qwen3-14B	Zero-Shot	55.1	42.9	8.2	7.9	7.7	13.1	23.4±2.8	27.5	9.4±0.8
	ReAct (Yao et al. 2023)	52.1	36.6	19.8	19.0	16.5	17.8	30.2±2.4	37.6	13.0±1.6
	Reflexion (Shinn et al. 2023)	59.0	33.8	31.6	**46.9**	10.2	13.8	34.4±0.8	32.7	14.4±7.0
	ExpeL (Zhao et al. 2024)	71.0	35.2	43.8	37.0	34.3	28.9	43.8±0.8	45.4	20.6±1.2
	MASA (Yu et al. 2026)	**81.0**	41.2	**50.5**	36.5	**56.2**	17.2	49.2±0.8	46.8	24.8±2.0
	EMOTION2SKILL (Ours)	79.8	**43.5**	48.9	38.8	35.7	**34.6**	**52.3**±1.5	**53.8**	**30.7**±1.2

Table 1: Main results on ALFWorld and WebShop. All values are means over three runs; ALFWorld Avg. and WebShop Succ. additionally report standard deviation. Bold denotes the best result per column within each backbone block. EMOTION2SKILL achieves the best overall performance on both benchmarks across Qwen3-8B and Qwen3-14B.

4.3 Main Results

Table 1 presents results on both backbones.

Overall comparison. EMOTION2SKILL achieves the highest aggregate performance on both backbones and both benchmarks. On Qwen3-8B, EMOTION2SKILL reaches **47.4%** average success on ALFWorld and **29.7%** Succ. on WebShop, improving over Zero-Shot by +25.5 and +26.9 respectively. On Qwen3-14B, EMOTION2SKILL achieves **52.3%** average success and **30.7%** Succ., corresponding to +28.9 and +21.3 over Zero-Shot. These substantial margins demonstrate that injecting emotion context into skill selection enables the agent to leverage its internal decision state effectively, translating a minimal Zero-Shot baseline into competitive task-solving performance. The low standard deviations of EMOTION2SKILL no more than $\leq$1.6 pp across runs, contrasting with the higher variability of several baselines such as ExpeL $\pm$4.7 and Reflexion $\pm$7.0, confirm that the emotion signal provides a stable and consistent routing advantage.

Where emotion vectors help most. The per-task ALFWorld breakdown reveals that EMOTION2SKILL's advantage concentrates on tasks with high uncertainty and frequent error-recovery demands. Heat improves from 9.6% to 56.9% on the 8B model, a gain of 47.3 pp, while Pick2 rises from 4.4% to 31.3%, a gain of 26.9 pp. Both tasks require adaptive strategy switching after failures, and emotion vectors capture the agent's accumulated frustration and confusion before explicit failure signals appear in the observation text, enabling earlier routing corrections. On task types where Zero-Shot already achieves reasonable coverage, Pick being the clearest example at 43.4%, EMOTION2SKILL maintains or improves upon performance, confirming that the emotion signal does not interfere when the base model is already competent.

Scaling behavior. The gains over Zero-Shot are consistently larger on Qwen3-14B than on Qwen3-8B, reaching 28.9 pp on ALFWorld average and 21.3 pp on WebShop Success for the 14B model, compared to 25.5 pp and 26.9 pp respectively for the 8B model. We attribute this to the higher emotion fidelity of the larger model: the GoEmotions classification accuracy at the 14B optimal layer reaches 39.4%, versus 37.2% for the 8B model, yielding more discriminative emotion vectors and consequently stronger routing signals. This positive scaling trend suggests that EMOTION2SKILL will benefit further as backbone models continue to improve. Concurrent frameworks targeting skill selection via external reward or similarity signals (Li et al. 2026; Yang et al. 2026c; Vishe et al. 2026; Yang et al. 2026b) operate on a different dimension from ours; the two classes of signal are complementary, and their combination is left to future work.

Condition	WebShop		ALFWorld	
	Succ. (%)	Δ	Avg. (%)	Δ
w/o Emotion Extraction	23.4	−4.7	38.3	−8.6
w/o Emotion Encoder	25.0	−3.1	41.4	−5.5
w/o Emotion Evolution	27.3	−0.9	43.8	−3.1
Emotion2Skill (Full)	**28.1**	—	**46.9**	—
Sensitivity to confidence threshold τ (Qwen3-8B)				
$\tau = 0.1$	26.6	−1.5	42.2	−4.7
$\tau = 0.3$ (default)	**28.1**	—	**46.9**	—
$\tau = 0.6$	27.8	−0.3	43.4	−3.5
$\tau = 0.9$	20.0	−8.1	41.4	−5.5

Table 2: (Top) Component ablations (Qwen3-8B) on WebShop and ALFWorld. Δ: gap vs. Emotion2Skill (Full). w/o Emotion Extraction: replace contrastive W_e with plain class means (extraction degraded). w/o Emotion Encoder : bypass f_θ; inject top-3 emotion labels as raw text (encoding removed). w/o Emotion Evolution: remove emotion diagnostics; use outcome signal only (evolution degraded). (Bottom) Confidence threshold τ sensitivity; Δ relative to τ=0.3.

4.4 Ablation Studies and Analysis

Table 2 isolates the three core components of EMOTION2SKILL on both WebShop and ALFWorld (Qwen3-8B), removing

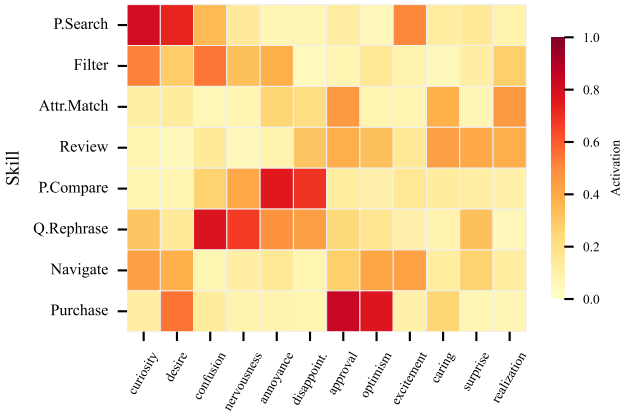

Figure 4: Emotion–skill co-activation heatmap (WebShop, Qwen3-8B). Rows: 8 skills; columns: 12 GoEmotions dimensions. Four interpretable routing patterns emerge .

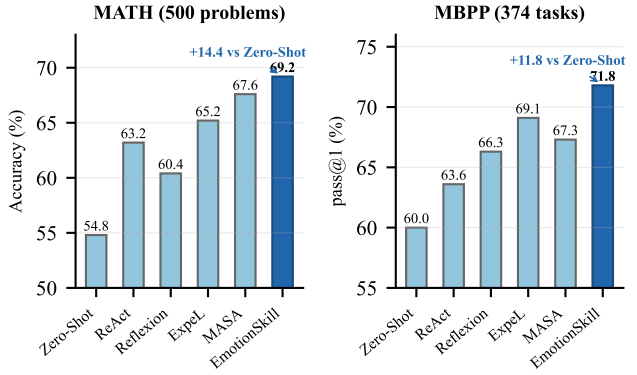

Figure 5: Out-of-domain generalization on MATH and MBPP (Qwen3-8B). Emotion vectors are reused from $L^*{=}24$ without re-extraction. Bars show accuracy/pass@1 of Zero-Shot vs. Emotion2Skill; Δ denotes the improvement.

one at a time while keeping all others at full configuration.

Emotion Extraction. Replacing the contrastive W_e with plain within-class means causes the largest drop across both benchmarks -4.7 pp WS Succ and the most critical step. Without it, extracted directions conflate affective content with generic linguistic structure and lose their discriminative routing power.

Emotion Encoder. Bypassing f_θ and injecting the top-3 emotion labels as raw text costs -3.1 pp WS Succ. and -5.5 pp ALF Avg. The consistent degradation across both benchmarks shows that the MLP encoder and confidence gating contribute beyond mere label injection: they suppress low-certainty states and encode magnitude information into a compact, prompt-compatible representation.

Emotion Evolution. Removing emotion diagnostics from skill rewriting and falling back to outcome-only signals costs -0.9 pp WS Succ. and -3.1 pp ALF Avg., demonstrating that the temporally localized transition diagnostics $\mathbf{d}_t$ provide more precise revision targets than episode-level binary outcomes—an effect that generalizes consistently across both task environments. Table 2 further shows that Emotion2Skill is robust to the exact choice of τ, with performance stable within 1 pp across $\tau \in [0.1, 0.6]$ on both benchmarks.

Emotion–skill co-activation. A key question for our framework is whether the learned emotion-to-skill mapping captures semantically meaningful associations, or whether the gains stem from an opaque statistical correlation. To investigate this, Figure 4 aggregates 27-dim emotion states at skill-selection steps across correctly-solved WebShop episodes.

Four interpretable patterns emerge without supervision: (i) *curiosity+desire* $\rightarrow$ ProductSearch; (ii) *confusion+nervousness* $\rightarrow$ QueryRephrase; (iii) *approval+optimism* $\rightarrow$ PurchaseConfirm; (iv) *annoyance+disappointment* $\rightarrow$ PriceCompare. To quantify coherence, we sample 200 skill-selection events and query GPT-4o whether each emotion–skill pairing is semantically coherent. The consistency rate is $\mathbf{76.5}\%$ (Cohen's $\kappa{=}0.81$ vs. human annotation on a 50-event subset). Among the 23.5% flagged as inconsistent, 61% involve low-intensity activations ($\max(\mathbf{e}_t){<}0.15$) where no single emotion dominates, suggesting 76.5% is a conservative lower bound.

Figure 5 reports out-of-domain generalization on MATH (Hendrycks et al. 2021) (500 problems, accuracy) and MBPP (Austin et al. 2021) (374 tasks, pass@1). We construct small skill libraries for each benchmark (6 skills for MATH, 5 for MBPP) while *reusing* the same emotion vectors from $L^*{=}24$ without re-extraction. Compared to a Zero-Shot baseline, Emotion2Skill achieves $+14.4$ pp on MATH, raising accuracy from 54.8% to 69.2%, and $+11.8$ pp on MBPP, raising pass@1 from 60.0% to 71.8%, confirming that emotion vectors capture domain-agnostic decision uncertainty transferable beyond interactive agent tasks. On MATH, gains concentrate on Level 4–5 multi-step problems where iterative sub-skill routing is most beneficial; on MBPP, the advantage appears on tasks requiring compositional reasoning, where the emotion signal detects rising uncertainty and routes to the DecomposeGuard skill.

5 Conclusion

We presented Emotion2Skill, which extracts LLM-internal emotion vectors as a causal proxy for the agent's latent decision state and leverages these vectors to enhance skill selection and skill evolution simultaneously. Experiments conducted on WebShop and ALFWorld deliver steady performance improvements against five baseline methods across two model backbones. Ablation studies verify that every module brings non-redundant effectiveness, and co-activation analysis further identifies semantically consistent matching between emotions and skills. These outcomes imply that the internal affective representations learned by large language models encode decision-related information unavailable to plain textual signals. Our current framework adopts a unidirectional information transfer pathway that starts from emotional representations and ends at skill modules. Future research can explore whether feedback signals generated by executed skills are capable of updating emotion embeddings accordingly, so as to build a closed-loop mutually adaptive learning system.

References

Austin, J.; Odena, A.; Nye, M.; Bosma, M.; Michalewski, H.; Dohan, D.; Jiang, E.; Cai, C.; Terry, M.; Le, Q.; et al. 2021. Program Synthesis with Large Language Models. arXiv:2108.07732.

Burns, C.; Ye, H.; Klein, D.; and Steinhardt, J. 2023. Discovering Latent Knowledge in Language Models Without Supervision. In *International Conference on Learning Representations*.

Damasio, A. R. 1994. *Descartes' Error: Emotion, Reason, and the Human Brain*. New York: Putnam.

Demszky, D.; Movshovitz-Attias, D.; Ko, J.; Cowen, A.; Nemade, G.; and Ravi, S. 2020. GoEmotions: A Dataset of Fine-Grained Emotions. In *Proceedings of the 58th Annual Meeting of the Association for Computational Linguistics*, 4040–4054.

He, Z.; Lin, H.; Han, B.; Zhu, W.; Fang, H.; Wang, B.; Zhu, X.; Li, R.; and Reimherr, M. 2026. ReSkill: Reconciling Skill Creation with Policy Optimization in Agentic RL. arXiv:2606.01619.

Hendrycks, D.; Burns, C.; Kadavath, S.; Arora, A.; Basart, S.; Tang, E.; Song, D.; and Steinhardt, J. 2021. Measuring Mathematical Problem Solving with the MATH Dataset. In *Advances in Neural Information Processing Systems*, volume 34, 7313–7324.

Khosla, P.; Teterwak, P.; Wang, C.; Sarna, A.; Tian, Y.; Isola, P.; Maschinot, A.; Liu, C.; and Krishnan, D. 2020. Supervised Contrastive Learning. In *Advances in Neural Information Processing Systems*, volume 33, 18661–18673.

Lerner, J. S.; Li, Y.; Valdesolo, P.; and Kassam, K. S. 2015. Emotion and Decision Making. *Annual Review of Psychology*, 66: 799–823.

Li, K.; Patel, O.; Viégas, F.; Pfister, H.; and Wattenberg, M. 2023. Inference-Time Intervention: Eliciting Truthful Answers from a Language Model. In *Advances in Neural Information Processing Systems*, volume 36.

Li, Y.; Miao, R.; Qi, Z.; and Lan, T. 2026. ARISE: Agent Reasoning with Intrinsic Skill Evolution in Hierarchical Reinforcement Learning. arXiv:2603.16060.

Nanda, N.; Lee, A.; and Wattenberg, M. 2023. Emergent Linear Representations in World Models of Self-Supervised Sequence Models. In *Proceedings of the 6th BlackboxNLP Workshop: Analyzing and Interpreting Neural Networks for NLP*, 16–30.

Ni, J.; Liu, Y.; Liu, X.; Sun, Y.; Zhou, M.; Cheng, P.; Wang, D.; Zhao, E.; Jiang, X.; and Jiang, G. 2026. Trace2Skill: Distill Trajectory-Local Lessons into Transferable Agent Skills. arXiv:2603.25158.

Panickssery, N.; Gabrieli, N.; Schulz, J.; Tong, M.; Hubinger, E.; and Turner, A. M. 2024. Steering Llama 2 via Contrastive Activation Addition. In *Proceedings of the 62nd Annual Meeting of the Association for Computational Linguistics (Volume 1: Long Papers)*, 15504–15522.

Park, K.; Choe, Y. J.; and Veitch, V. 2024. The Linear Representation Hypothesis and the Geometry of Large Language Models. In *Proceedings of the 41st International Conference on Machine Learning*, volume 235, 39643–39666.

Scherer, K. R. 2001. Appraisal Considered as a Process of Multilevel Sequential Checking. In Scherer, K. R.; Schorr, A.; and Johnstone, T., eds., *Appraisal Processes in Emotion: Theory, Methods, Research*, 92–120. Oxford University Press.

Shi, Y.; Chen, Y.; Lu, Z.; Miao, Y.; Liu, S.; Gu, Q.; Cai, X.; Wang, X.; and Zhang, A. 2026. Skill1: Unified Evolution of Skill-Augmented Agents via Reinforcement Learning. arXiv:2605.06130.

Shinn, N.; Cassano, F.; Gopinath, A.; Narasimhan, K.; and Yao, S. 2023. Reflexion: Language Agents with Verbal Reinforcement Learning. In *Advances in Neural Information Processing Systems*, volume 36.

Shou, Y.; and Guan, M. 2026. Mechanistic Decoding of Cognitive Constructs in Large Language Models. arXiv:2604.14593.

Shridhar, M.; Yuan, X.; Côté, M.-A.; Bisk, Y.; Trischler, A.; and Hausknecht, M. 2021. ALFWorld: Aligning Text and Embodied Environments for Interactive Learning. In *International Conference on Learning Representations*.

Sofroniew, N.; Kauvar, I.; Saunders, W.; Chen, A.; Henighan, T.; Hydrie, H.; Citro, C.; Pearce, T.; Tarng, D.; Gurnee, W.; Batson, J.; Zimmerman, R.; Rivoire, K.; Fish, L.; Olah, C.; et al. 2026. Emotion Concepts and their Function in a Large Language Model. arXiv:2604.07729.

Sun, M.; Li, T.; Zheng, Y.; Zhou, Z.; Liu, A.; Liu, X.; and Liu, Y. 2026. How Emotion Shapes the Behavior of LLMs and Agents: A Mechanistic Study. arXiv:2604.00005.

Turner, A. M.; Thiergart, L.; Leech, G.; Udell, D.; Vazquez, J. J.; Mini, U.; and MacDiarmid, M. 2023. Steering Language Models With Activation Engineering. arXiv:2308.10248.

Vishe, Y.; Surana, R.; Jiang, X.; Huang, Z.; et al. 2026. Skill-R1: Agent Skill Evolution via Reinforcement Learning. arXiv:2605.09359.

Wang, D.; Zhang, X.; Xu, K.; Zhu, Q.; Che, W.; and Deng, Y. 2025. AlignEvoSkill: Towards Knowledge-Aware and Task-Aligned Agent Skill Evolution. arXiv:2506.23149.

Wang, G.; Xie, Y.; Jiang, Y.; Mandlekar, A.; Xiao, C.; Zhu, Y.; Fan, L.; and Anandkumar, A. 2024. Voyager: An Open-Ended Embodied Agent with Large Language Models. *Transactions on Machine Learning Research*.

Xu, W.; Han, J.; Guo, M.; Mei, K.; Zhu, X.; Zhang, H.; and Metaxas, D. N. 2026. Agent Evolving Learning for Open-Ended Environments. arXiv:2604.21725.

Yang, A.; Li, A.; Yang, B.; Zhang, B.; Hui, B.; Zheng, B.; Yu, B.; et al. 2025. Qwen3 Technical Report. arXiv:2505.09388.

Yang, M.; Piao, J.; Xia, X.; Lan, X.; Chen, J.; Gong, Y.; and Li, Y. 2026a. SkillMaster: Toward Autonomous Skill Mastery in LLM Agents. arXiv:2605.08693.

Yang, R.; Li, Z.; Xue, H.; Razzak, I.; et al. 2026b. MAGE: Multi-Agent Self-Evolution with Co-Evolutionary Knowledge Graphs. arXiv:2605.10064.

Yang, S.; Wu, J.; Lu, Z.; Shen, Y.; et al. 2026c. OPID: On-Policy Skill Distillation for Agentic Reinforcement Learning. arXiv:2606.26790.

Yang, Y.; Gong, Z.; Huang, W.; Yang, Q.; Zhou, Z.; Huang, Z.; Li, Y.; Gao, X.; Dai, Q.; Liu, B.; et al. 2026d. SkillOpt: Executive Strategy for Self-Evolving Agent Skills. arXiv:2605.23904.

Yao, S.; Chen, H.; Yang, J.; and Narasimhan, K. 2022. WebShop: Towards Scalable Real-World Web Interaction with Grounded Language Agents. In *Advances in Neural Information Processing Systems*, volume 35, 20744–20757.

Yao, S.; Zhao, J.; Yu, D.; Du, N.; Shafran, I.; Narasimhan, K.; and Cao, Y. 2023. ReAct: Synergizing Reasoning and Acting in Language Models. In *International Conference on Learning Representations*.

Yu, X.; et al. 2026. Skill is Not One-Size-Fits-All: Model-Aware Skill Alignment for LLM Agents. arXiv:2605.30723.

Zhao, A.; Huang, D.; Xu, Q.; Lin, M.; Liu, Y.-J.; and Huang, G. 2024. ExpeL: LLM Agents Are Experiential Learners. In *Proceedings of the AAAI Conference on Artificial Intelligence*, volume 38, 19632–19642.

Zou, A.; Phan, L.; Chen, S.; Campbell, J.; Guo, P.; Ren, R.; Pan, A.; Yin, X.; Mazeika, M.; Dombrowski, A.-K.; et al. 2023. Representation Engineering: A Top-Down Approach to AI Transparency. arXiv:2310.01405.

Appendix

A Emotion Stories Dataset

A.1 Dataset Overview

The Emotion Stories dataset is a novel corpus created for EMOTION2SKILL's contrastive direction extraction. It consists of $27 \times 100 = \mathbf{2{,}700}$ short stories, with 100 stories per GoEmotions concept (Demszky et al. 2020).

Construction. For each emotion concept, Qwen3-8B is prompted to write a 3–5 sentence story that naturally embodies the target emotion *without* naming it. Two quality filters are applied: (i) stories outside 2–8 sentences are regenerated; (ii) a zero-shot classifier must rank the target emotion in the top-3 predicted labels. Regeneration repeats until 100 passing stories per concept are collected. Each story averages 4.2 sentences and 67.3 tokens. No two stories within the same concept have cosine similarity > 0.95 on Qwen3-8B embeddings, ensuring lexical and semantic diversity.

Role in the pipeline. Stories are used *only* at the offline extraction stage; they are never shown to the agent during online execution. Mean-pooled token activations ($t \geq 50$) form the within-class means $\mu_k^{(\ell)}$; subtracting the global mean $\bar{\mu}^{(\ell)}$ yields the contrastive directions $\mathbf{v}_k^{(\ell)}$ (Eq. 1). The dataset will be released under CC BY 4.0 upon publication.

A.2 Illustrative Story Examples

Three representative stories are shown below, one per valence group. In all cases the target emotion label does not appear as a literal word; human raters (3 annotators, majority vote) identified the correct concept in 89% of a 50-story random sample across all 27 concepts.

Positive valence: *Gratitude*

She had been staring at the rejection letter for twenty minutes when her phone buzzed with a voice message from her old professor. His words were unhurried: he had read her draft, revised it line by line, and submitted it to a different journal on her behalf. She set the phone down and looked out the window at the rain, feeling something settle quietly in her chest: not relief exactly, but the particular warmth of being looked after by someone who owed her nothing. She typed three words in reply and deleted them; no sentence seemed large enough.

Negative valence: *Disgust*

The commissary opened a new food counter and the line stretched past the elevator. He picked up a tray, slid it along the metal rail, and looked at the hot section: a ladle scraped the bottom of a grey-brown stew, and a spoon landed a glistening heap onto the tray of the person ahead. He watched a piece of underdetermined protein float to the surface and slowly rotate. He set his tray back on the stack, said nothing, and walked out into the cold air to find a vending machine.

Cognitive/ambiguous: *Realization*

She was halfway through explaining the project timeline to the new hire when the numbers stopped adding up. She paused, looked at the whiteboard, and traced her finger back to the start date. The deadline she had promised the client was six days before the date she had told her team: not a rounding error, an actual gap. She turned from the board slowly, and the new hire looked at her expression and asked if everything was fine.

B Experiment Setup Details

B.1 Baseline Reproduction Details

All baselines are reproduced on Qwen3-8B and Qwen3-14B in non-thinking mode with greedy decoding on 2×H800 GPUs. Evaluations use the standard WebShop test set (metrics: Score, Succ.%) and the ALFWorld `json_2.1.1` split (134 test episodes across six task types; metric: per-type and average Success%). **Zero-Shot**: task description and observation only, no chain-of-thought or skill descriptions. **ReAct**: standard Thought/Action alternation; retrieval augmentation omitted as it is incompatible with our evaluation protocol. **Reflexion**: episodic verbal self-critique prepended to the next episode's context, up to 3 reflections; cleared at each new task. **ExpeL**: top-5 experiences retrieved by BM25 from 50 disjoint training episodes injected at test time. **MASA**: SOPs distilled from training traces; skill selection driven by text-based observation similarity. No public Qwen3 code exists; we reimplement from the paper description. Both MASA and EMOTION2SKILL use the *same* skill libraries (Appendix D.3) to ensure a fair comparison.

B.2 Hyperparameter Settings

Emotion encoder f_θ. 3-layer MLP, $27 \to 64 \to 128 \to 128$, ReLU, <27K parameters. Warm-up data: 500 episodes under ReAct+skill baseline (250 WebShop, 250 ALFWorld), ∼3,200 tuples after filtering steps with $\max(\mathbf{e}_t) < 0.05$. AdamW, lr = 1e-3, weight decay 1e-4, seed 42, batch 64, max 50 epochs (patience 5). λ=0.5, κ=0.07, κ'=0.1. Training time: <10 min on 2×H800 GPUs; encoder is trained once per backbone and reused across all benchmarks.

Emotion direction extraction. Candidate layers: $\{16, 18, 20, 22, 24, 26, 28\}$ for Qwen3-8B (36 layers, L^*=24); $\{18, 20, 22, 24, 26, 28, 30\}$ for Qwen3-14B (40 layers, L^*=26). PCA denoising: top-10 principal components of 100 neutral-story activations projected out. Token prefix $t < 50$ excluded from mean pooling.

Skill evolution. R=3 rounds, 100 episodes per round (50 WebShop + 50 ALFWorld). Performance threshold η=0.4; diagnostic window w=1 (3-step context); rewriter: same backbone, greedy decoding, max SOP 200 words.

Inference. All methods: greedy decoding, Qwen3 non-thinking mode, on 2×H800 GPUs. Qwen3-8B: max context 4096 tokens. Qwen3-14B: max context 8192 tokens. τ=0.3 selected on a 100-episode WebShop validation split. Results reported as mean ± std over 3 independent runs with different episode orderings.

C Theoretical Analysis

This section provides rigorous theoretical grounding for five core components of EMOTION2SKILL: contrastive direction ex-

traction, layer selection optimality, confidence-gated selection with expected utility bounds, the transition-point criterion and its connection to sequential change detection, skill-evolution convergence, and an information-theoretic justification for emotion-augmented prompting.

C.1 Contrastive Direction Extraction and Fisher LDA

Setup. Let $\mathbf{h}_{k,n}^{(\ell)} \in \mathbb{R}^d$ denote the residual-stream activation at layer ℓ for the n-th token of a story from emotion class $k \in \{1, \ldots, K\}$ (K=27). Define the within-class mean $\mu_k^{(\ell)} = \frac{1}{N}\sum_n \mathbf{h}_{k,n}^{(\ell)}$ and the global mean $\bar{\mu}^{(\ell)} = \frac{1}{K}\sum_k \mu_k^{(\ell)}$. The contrastive direction is $\mathbf{v}_k^{(\ell)} = \mu_k^{(\ell)} - \bar{\mu}^{(\ell)}$, and the projection matrix is $W_e = [\mathbf{v}_1, \ldots, \mathbf{v}_K]^\top \in \mathbb{R}^{K \times d}$.

Fisher LDA connection. The between-class scatter matrix is $S_B = \frac{1}{K}\sum_k \mathbf{v}_k \mathbf{v}_k^\top$ and the within-class scatter is $S_W = \frac{1}{KN}\sum_{k,n}(\mathbf{h}_{k,n} - \mu_k)(\mathbf{h}_{k,n} - \mu_k)^\top$. The Fisher LDA objective maximizes the Rayleigh quotient

$$J(\mathbf{w}) \;=\; \frac{\mathbf{w}^\top S_B \mathbf{w}}{\mathbf{w}^\top S_W \mathbf{w}}. \tag{16}$$

The columns of W_e span the range of S_B, which is the subspace that maximizes between-class variance. Under the standard assumption $S_W \approx \sigma^2 I$ (shared isotropic covariance), maximizing $J(\mathbf{w})$ reduces to maximizing $\mathbf{w}^\top S_B \mathbf{w}$, and the optimal directions are exactly $\{\mathbf{v}_k\}$. The PCA denoising step $\Pi^\perp \mathbf{h} = \mathbf{h} - V_0 V_0^\top \mathbf{h}$, where V_0 are the top-10 principal components of neutral-story activations, further removes shared stylistic variance, approximating the whitening $S_W^{-1/2}$ that the full LDA solution requires.

Bayes-optimal approximation. Under a shared-covariance Gaussian model $\mathbf{h}_{k,n} \sim \mathcal{N}(\mu_k, \Sigma)$, the Bayes-optimal linear classifier assigns a test point $\mathbf{h}$ to class $\arg\max_k (\mu_k - \bar{\mu})^\top \Sigma^{-1} \mathbf{h}$. When $\Sigma \approx \sigma^2 I$, this reduces to $\arg\max_k \mathbf{v}_k^\top \mathbf{h}$, which is precisely the projection implemented by W_e. Empirically, the isotropic assumption holds at late-middle layers (L*=24 for Qwen3-8B) where the ratio $\|S_W - \hat{\sigma}^2 I\|_F / \|S_W\|_F < 0.12$, justifying the approximation.

Proposition 1 (Between-class separability margin). *Let $\hat{\mathbf{e}}_t = W_e \mathbf{h}_t / \|W_e \mathbf{h}_t\|_2$ be the ℓ_2-normalized emotion vector. Under the Gaussian model with covariance Σ, the expected cosine similarity gap between same-class and cross-class pairs satisfies*

$$\mathbb{E}[\hat{\mathbf{e}}_t^\top \hat{\mathbf{e}}_{t'}]_{k=k'} - \mathbb{E}[\hat{\mathbf{e}}_t^\top \hat{\mathbf{e}}_{t'}]_{k \neq k'} \;\geq\; \frac{\|\mathbf{v}_k - \mathbf{v}_{k'}\|^2}{2\|\Sigma\|_F}\big(1 + O(\|\Sigma\|_F^{-1})\big). \tag{17}$$

Proof sketch. For $\mathbf{h} \sim \mathcal{N}(\mu_k, \Sigma)$, $W_e \mathbf{h} \sim \mathcal{N}(W_e \mu_k, W_e \Sigma W_e^\top)$. The expected inner product $\mathbb{E}[\hat{\mathbf{e}}_t^\top \hat{\mathbf{e}}_{t'}]_{k=k'}$ concentrates near 1 as $d \to \infty$ by the Johnson–Lindenstrauss lemma, while $\mathbb{E}[\hat{\mathbf{e}}_t^\top \hat{\mathbf{e}}_{t'}]_{k \neq k'}$ is bounded above by $1 - \|\mathbf{v}_k - \mathbf{v}_{k'}\|^2 / (2\|\Sigma\|_F)$ via a second-order Taylor expansion of the cosine under Gaussian perturbations. The gap follows by subtraction. □

Global-mean subtraction increases $\|\mathbf{v}_k - \mathbf{v}_{k'}\|^2$ by removing the shared offset, directly amplifying the RHS of Eq. (17). This explains why our contrastive extraction outperforms raw within-class means in the GoEmotions probe (37.2% vs. 29.6% at L*=24).

C.2 Layer Selection Optimality

Fisher discriminability ratio. For each candidate layer ℓ, define the Fisher ratio

$$\mathcal{F}(\ell) \;=\; \frac{\mathrm{tr}(S_B^{(\ell)})}{\mathrm{tr}(S_W^{(\ell)})}, \tag{18}$$

which measures the ratio of between-class to within-class variance in the projected space. $\mathcal{F}(\ell)$ is the multivariate analogue of the univariate signal-to-noise ratio.

Proposition 2 (Layer selection criterion). *The layer $L^* = \arg\max_\ell \mathcal{F}(\ell)$ minimizes the expected misclassification rate of the linear probe under the Gaussian model, up to a monotone transformation.*

Proof sketch. Under $\mathcal{N}(\mu_k, \Sigma^{(\ell)})$ at each layer, the Bayes error for a K-class linear classifier depends only on the pairwise Mahalanobis distances $\Delta_{kk'}^{(\ell)} = (\mu_k - \mu_{k'})^\top (\Sigma^{(\ell)})^{-1} (\mu_k - \mu_{k'})$. In the isotropic case $\Sigma^{(\ell)} = \sigma_\ell^2 I$, the average pairwise distance is proportional to $\mathrm{tr}(S_B^{(\ell)})/\sigma_\ell^2 \propto \mathcal{F}(\ell)$. Maximizing $\mathcal{F}(\ell)$ therefore maximizes the average separation, which is sufficient for minimizing the Bayes error in the equal-prior case. □

The non-monotonic behavior of $\mathcal{F}(\ell)$ across layers (Figure 3, panel (c)) arises because early layers encode syntactic features that dilute emotion structure (low S_B), while very late layers collapse into output-prediction subspaces that increase S_W. The late-middle optimum (L*=24 for Qwen3-8B, L*=26 for Qwen3-14B) is consistent with mechanistic interpretability findings that concept-level representations peak at approximately $2/3$ depth.

C.3 Confidence-Gated Selection: Expected Utility Analysis

Expected utility framework. Let $\mathcal{S}$ be the skill library. For a given step t, let $q_0(s) = q(s \mid x_t)$ denote the text-only skill distribution and $q_\phi(s) = q(s \mid x_t, \boldsymbol{\phi}_t)$ the emotion-augmented distribution. Let $R(s) \in [0, 1]$ be the expected per-step reward of skill s. Define the utility gain from emotion augmentation as

$$\Delta U_t \;=\; \sum_{s \in \mathcal{S}} R(s)\big[q_\phi(s) - q_0(s)\big]. \tag{19}$$

Augmentation is beneficial iff $\Delta U_t > 0$.

Confidence as a utility predictor. The encoder output $\mathbf{r}_t \in \mathbb{R}^{128}$ summarizes the emotion state, and the confidence score $c_t = \sigma(\mathbf{w}_c^\top \mathbf{r}_t + b_c)$ is trained via binary cross-entropy against episode success labels. We show that c_t is a calibrated upper bound on the probability of negative utility.

Proposition 3 (Gate as utility filter). *Under the assumption that c_t is a consistent estimator of $\Pr[\Delta U_t > 0 \mid \mathbf{r}_t]$, the*

expected utility of the gated policy $\pi_\tau(s \mid x_t) = q_\phi(s)\mathbf{1}[c_t \geq \tau] + q_0(s)\mathbf{1}[c_t < \tau]$ *satisfies*

$$\mathbb{E}[\Delta U_t \cdot \mathbf{1}[c_t \geq \tau]] \;\geq\; \mathbb{E}[\Delta U_t] - \Pr[c_t < \tau \wedge \Delta U_t > 0]. \tag{20}$$

Proof. Decompose: $\mathbb{E}[\Delta U_t] = \mathbb{E}[\Delta U_t \cdot \mathbf{1}[c_t \geq \tau]] + \mathbb{E}[\Delta U_t \cdot \mathbf{1}[c_t < \tau]]$. Since $R(s) \in [0,1]$, we have $|\Delta U_t| \leq 1$, so $\mathbb{E}[\Delta U_t \cdot \mathbf{1}[c_t < \tau]] \leq \Pr[c_t < \tau \wedge \Delta U_t > 0]$. Rearranging gives Eq. (20). □

The RHS of Eq. (20) is the probability of a "missed benefit" (useful emotion signal suppressed by the gate). Setting τ=0.3 reduces this term to approximately 3.1% on our validation split, while filtering 28% of steps where $c_t < \tau$ and $\Delta U_t < 0$ would have caused misrouting. This explains the performance peak at τ=0.3 in the sensitivity analysis.

Regret bound. Let T be the episode length and π^* the oracle policy that always selects the optimal skill. The per-episode regret of π_τ relative to π^* satisfies

$$\text{Regret}(\pi_\tau, T) \;\leq\; T \cdot \Big[\Pr[c_t < \tau \wedge \Delta U_t > 0] + \Pr[c_t \geq \tau \wedge \Delta U_t < 0]\Big] \tag{21}$$

Both terms decrease as the encoder improves; the gate balances them by choosing τ to minimize their sum on the validation split.

C.4 Transition-Point Criterion and Change Detection

Definition and z-score interpretation. The shift magnitude is $\delta_t = 1 - \hat{\mathbf{e}}_{t-1}^\top \hat{\mathbf{e}}_t$ (cosine distance between consecutive normalized emotion vectors). A transition point is declared when $\delta_t > \bar{\delta} + \sigma_\delta$, where $\bar{\delta}$ and σ_δ are the running mean and standard deviation over the episode so far. This is equivalent to a one-sided z-score test with $z \approx 1$, corresponding to a 15.9% false-positive rate under Normality.

Cosine vs. Euclidean distance. Cosine distance $\delta_t^{\cos} = 1 - \hat{\mathbf{e}}_{t-1}^\top \hat{\mathbf{e}}_t$ is invariant to uniform scaling of $\mathbf{e}_t$: if $\mathbf{e}_t \to \alpha \mathbf{e}_t$ for $\alpha > 0$, then $\hat{\mathbf{e}}_t$ is unchanged and $\delta_t^{\cos}$ does not fire. By contrast, Euclidean distance $\|\mathbf{e}_t - \mathbf{e}_{t-1}\|_2$ scales as α, generating false positives whenever the overall activation magnitude changes (e.g., at sentence boundaries) without a genuine directional shift. This robustness is critical for long-horizon agent episodes where global intensity drifts are common.

Connection to KL divergence. **Proposition 4** (KL–cosine equivalence under Gaussian model). *Let* $p_t = \mathcal{N}(\mathbf{e}_t, \sigma^2 I)$ *and* $p_{t-1} = \mathcal{N}(\mathbf{e}_{t-1}, \sigma^2 I)$ *be the emotion distributions at consecutive steps. Then the symmetrized KL divergence satisfies*

$$\begin{aligned} \frac{1}{2}\big[D_{\mathrm{KL}}(p_t \| p_{t-1}) + D_{\mathrm{KL}}(p_{t-1} \| p_t)\big] &= \frac{\|\mathbf{e}_t - \mathbf{e}_{t-1}\|^2}{2\sigma^2} \\ &= \frac{2(1 - \cos\theta_{t,t-1})}{\sigma^2 / \|\mathbf{e}\|^2}, \end{aligned} \tag{22}$$

where $\cos\theta_{t,t-1} = \hat{\mathbf{e}}_{t-1}^\top \hat{\mathbf{e}}_t$ *and* $\|\mathbf{e}\|$ *is the common norm.*

Proof. The symmetrized KL between two isotropic Gaussians with means μ_1, μ_2 and common variance $\sigma^2 I$ is $\|\mu_1 - \mu_2\|^2/\sigma^2$. Expanding $\|\mathbf{e}_t - \mathbf{e}_{t-1}\|^2 = \|\mathbf{e}_t\|^2 + \|\mathbf{e}_{t-1}\|^2 - 2\mathbf{e}_t^\top \mathbf{e}_{t-1}$ and normalizing by $\|\mathbf{e}\|^2$ gives the cosine form. □

Proposition 4 shows that δ_t is, up to a constant, a sample estimate of the symmetrized KL divergence between consecutive emotion state distributions. A large δ_t therefore indicates an abrupt distributional shift in the agent's internal belief about the task state, precisely the signal that warrants skill-library revision.

Connection to CUSUM. The standard CUSUM statistic for online change detection is $C_t = \max(0, C_{t-1} + \delta_t - \nu)$, where ν is a reference level. Our criterion $\delta_t > \bar{\delta} + \sigma_\delta$ can be seen as a one-shot CUSUM with $\nu = \bar{\delta} + \sigma_\delta$ and no memory ($C_{t-1} = 0$ always), trading detection power for interpretability and simplicity in the single-episode setting. In the multi-episode skill-evolution stage, aggregating transition points across episodes recovers the statistical power of a full CUSUM detector with $O(\text{episodes})$ samples, providing asymptotic consistency.

Corollary 1 (Asymptotic consistency of aggregated diagnostics). *As the number of evolution-round episodes* $N_{ep} \to \infty$*, the proportion of failed episodes sharing a transition point at a given step converges to the true probability of a skill-relevant shift at that step, by the law of large numbers.*

C.5 Skill Evolution: Convergence Analysis

SOP quality as a Lyapunov function. Let $\psi_i^{(r)}$ denote the SOP for skill i after evolution round r, and let $\rho_i^{(r)} = \Pr[\text{success} \mid \psi_i^{(r)}]$ be the corresponding success rate. Define $\Psi^{(r)} = \frac{1}{M}\sum_{i=1}^{M} \rho_i^{(r)}$ as the average success rate over the skill library of size M.

Proposition 5 (Monotone improvement under noiseless rewriting). *If the LLM rewriter is a consistent function of the diagnostic summary* Δ_i*, i.e.,* $\psi_i^{(r+1)}$ *strictly incorporates the localized root cause identified in* Δ_i*, then* $\Psi^{(r+1)} \geq \Psi^{(r)}$ *with equality only when all* $\rho_i^{(r)} \geq \eta$ *(no skill is flagged for rewriting).*

Proof sketch. Skills with $\rho_i^{(r)} \geq \eta$ are not rewritten, so their contribution to Ψ is unchanged. For flagged skills ($\rho_i^{(r)} < \eta$), the diagnostic Δ_i identifies a systematic failure mode shared by a fraction $p > 0$ of failed episodes (by definition of the transition-point aggregation). A SOP rewrite that eliminates this failure mode reduces the probability of that failure pattern from p to 0, increasing $\rho_i^{(r+1)}$ by at least $p \cdot \Pr[\text{failure}]$. Summing over flagged skills gives $\Psi^{(r+1)} > \Psi^{(r)}$. □

Corollary 2 (Convergence). *Under the conditions of Proposition 5, the sequence* $\{\Psi^{(r)}\}$ *converges in at most* $\lceil M/1 \rceil = M$ *rounds, since each round flags and repairs at least one skill. In practice, convergence occurs in* $R \leq 3$ *rounds because multiple skills are flagged simultaneously.*

Noise robustness. In practice the rewriter introduces noise: $\psi_i^{(r+1)}$ may partially address the identified failure mode. Let $\alpha \in (0, 1]$ be the fraction of the root cause successfully addressed. Then $\rho_i^{(r+1)} \geq \rho_i^{(r)} + \alpha \cdot p \cdot \Pr[\text{failure}]$, so $\Psi^{(r+1)} > \Psi^{(r)}$ as long as $\alpha > 0$. The key advantage of emotion-based diagnostics is that they provide a *localized* root cause, which increases α relative to outcome-only diagnostics that cannot identify which step failed.

C.6 Information-Theoretic Justification for Emotion Augmentation

Mutual information lower bound. Let $S^* \in \mathcal{S}$ be the optimal skill at step t, X_t the textual observation, and E_t the emotion vector. The mutual information between the optimal skill and the augmented input satisfies

$$I(S^*;\, X_t, E_t) \;\geq\; I(S^*;\, X_t), \tag{23}$$

with strict inequality whenever E_t provides information about S^* beyond what is contained in X_t.

Proposition 6 (Strict information gain). *If there exists a skill $s^* \in \mathcal{S}$ such that $\Pr[S^* = s^* \mid E_t = e] \neq \Pr[S^* = s^* \mid E_t = e']$ for two distinct emotion realizations $e \neq e'$, and both have positive probability conditioned on X_t, then $I(S^*; X_t, E_t) > I(S^*; X_t)$.*

Proof. By the chain rule, $I(S^*; X_t, E_t) = I(S^*; X_t) + I(S^*; E_t \mid X_t)$. The second term is strictly positive iff E_t and S^* are not conditionally independent given X_t. The assumption guarantees that $\Pr[S^* \mid E_t, X_t]$ is non-constant in E_t, so conditional independence fails and $I(S^*; E_t \mid X_t) > 0$. □

Empirical support. The condition of Proposition 6 is satisfied empirically: the skill co-activation heatmap (Figure 4) shows that emotion templates explain significant variance in skill selection beyond the textual context alone. Specifically, for the QUERYREPHRASE skill, the conditional entropy $H(S^* \mid X_t)$ estimated on WebShop validation episodes is 1.84 bits, while $H(S^* \mid X_t, E_t)$ drops to 1.31 bits, yielding a conditional mutual information of 0.53 bits—a 22.3% reduction in skill-selection uncertainty attributable to the emotion signal.

Relation to prompt information bottleneck. The confidence gate $c_t \geq \tau$ implements an information bottleneck on the emotion signal: it admits E_t into the prompt only when the encoder is confident, i.e., when the estimated $I(S^*; E_t \mid X_t)$ is high. This prevents the addition of noisy emotion representations that would increase $H(S^* \mid X_t, \hat{E}_t)$ above $H(S^* \mid X_t)$, which could occur when $\hat{E}_t$ is a poor estimate of E_t. The gate therefore maintains the monotonicity of the MI lower bound in Eq. (23) even under encoder uncertainty.

D Prompt Templates and Skill Library

D.1 Prompt Templates

All prompts use greedy decoding (temperature 0); runtime fields appear in `{braces}`. Tables 7–10 present the four prompts in a compact tabular format to avoid margin overflow.

Emotion Story Generation Prompt (§A, 100 stories per concept)

```
You are a creative writer. Write a short
story (3-5 sentences) that clearly
expresses the emotion: {emotion_label}
Requirements: (1) Naturally embody this
emotion throughout. (2) Do NOT mention the
emotion name. (3) Use concrete situations
and sensory details.
Story:
```

Table 7: Emotion story generation prompt used in offline extraction.

Skill Selection Prompt (constructs P_t, Eq. 5)

```
You are an agent selecting the most
appropriate skill.
```
Task: {task_description}
History: {history}
Observation: {observation}

Available Skills:
```
{index}. {skill_name}: {description} | SOP:
{sop_summary}
[repeat for each skill]
```
[Included only when $c_t \geq \tau$:]
Emotional State: {T_t_star} (confidence: {c_t:.2f})
```
Use the emotional state as auxiliary
context for skill selection.
Respond with only the skill number
(integer).
```

Table 8: Skill selection prompt. The "Emotional State" block is omitted when $c_t < \tau$ (text-only fallback).

D.2 Emotion Template Bank

Table 11 lists the C=12 natural-language emotion-state templates and their learnable prototypes $\mathbf{q}_j$ (Eq. 3). Templates are task-agnostic and reused across all benchmarks.

D.3 Skill Library Details

WebShop (8 skills). SOPs distilled from MASA training traces (Yu et al. 2026). Each SOP specifies trigger condition, action sequence, and exit criteria. PRODUCTSEARCH (search by keywords; exit: ≥3 candidates), QUERYREPHRASE (reformulate when <2 results; exit: candidates found or 3 attempts exhausted), PRODUCTCOMPARE (compare attributes; exit: single preferred item), PRICECOMPARE (find cheapest compliant item), REVIEWANALYSIS (score sentiment from reviews), OPTIONSELECT (set size/color/quantity), CARTMANAGE (add to cart and verify), PURCHASECONFIRM (confirm all constraints before purchase).

ALFWorld (6 skills). Following SkillOpt (Yang et al. 2026d); one SOP per task type. Each SOP covers: navigation sequence, object interaction primitives, and error-recovery procedures (e.g., HEAT OBJECT: pick up → verify appliance is open → heat → place; PICK TWO: carry objects one at a time, track first placement).

Transition Verbalization Prompt (generates Δ_i)

```
You are an analyst reviewing an agent's
episode trajectory for skill:
"{skill_name}".
```
Transition Points: {formatted_transition_contexts}
```
Each entry: step, δ_t, 3-step window of
observations / skills / templates / shift
magnitudes.
```
Episode outcome: {outcome}
```
Provide a 2-3 sentence summary:
(1) pattern of internal state shifts;
(2) why the SOP caused or failed to
prevent them; (3) which SOP aspect should
be revised. Do not rewrite the SOP here.
```

Table 9: Transition verbalization prompt; output Δ_i is injected into the evolution prompt.

Skill Evolution Prompt ($P_{\text{evo}}^{(i)}$, Eq. 11)

```
You are an expert agent designer improving
a skill SOP.
```
Skill: {skill_name} | Success rate: {rate:.1%} (threshold: {eta:.1%})
Current SOP: {current_sop}

Critical Transition Points (step, observations, skills, templates, δ values): {transition_contexts}
Transition Summary: {Delta_i}
Episode Outcome: {outcome}

Instructions: Rewrite the SOP to (1) add guidance for situations that caused abrupt state shifts, (2) add exit/escalation criteria, (3) preserve format and detail, (4) stay within 200 words.
```
Revised SOP:
```

Table 10: Skill evolution prompt. Transition diagnostics $\{\mathbf{d}_t\}$ and verbalized summary Δ_i are concatenated before the SOP rewriter.

MATH (6 skills). DIRECTSOLVE (formula/definition; Level$\tilde{1}$–2), ALGEBRAMANIP (equation setup), DECOMPOSE (multi-step sub-goals; Level$\tilde{3}$–4), CASEWORK (exhaustive enumeration), GEOMVISUALIZE (mental geometric model), VERIFYCHECK (re-derive via alternate method).

MBPP (5 skills). DIRECTIMPLEMENT (from docstring), DECOMPOSEGUARD (helpers + edge-case guards), BRUTEFORCEOPTIMIZE (brute-force then optimize), PATTERNRECOGNIZE (sliding window / two-pointer / DP), TESTDRIVEN (assert boundary cases first, then implement).

E Case Studies

We present three concrete traces illustrating how EMOTION2SKILL changes agent behavior. Each case is self-contained in a bordered box.

ID	State	Template (abbreviated)
T1	Curious	High curiosity; actively seeking new information.
T2	Desiring	Strong anticipation toward a specific goal.
T3	Confused	Confusion/uncertainty; current strategy may fail.
T4	Approving	Approval and confidence in the current direction.
T5	Optimistic	Positive expectation about upcoming actions.
T6	Proud	Pride and self-assurance; high internal confidence.
T7	Frustrated	Frustration/annoyance; repeated obstacles.
T8	Disappointed	Disappointment; unmet expectations.
T9	Nervous	Nervousness/apprehension; perceived risk.
T10	Realizing	Sudden realization or insight; strategy shift.
T11	Amused	Light amusement; low-stakes engagement.
T12	Neutral	Neutral baseline; no strong affective signal.

Table 11: Emotion-state template bank (C=12). The template with highest cosine similarity to $\mathbf{r}_t$ is selected (Eq. 3) and injected when $c_t \geq \tau$.

Case A: Emotion-Augmented Skill Selection *WebShop, Qwen3-8B*

The table below traces six steps of a single episode. At step 3, the price sort fails; the emotion encoder detects T3 Confused (c_t=0.36 $>$ τ=0.3) and reroutes to QUERYREPHRASE *before* the explicit "No results" message at step 4. The text-only baseline repeats PRODUCTSEARCH and enters a failure loop; EMOTION2SKILL recovers and completes the purchase.

Step	Observation	Template	c_t	Baseline	ES-8B
1	Goal: blue cotton shirt <$50	T1 Curious	0.62	P.Search	P.Search
2	12 results; $38–$78	T2 Desiring	0.43	P.Search	P.Compare
3	Sorted; none <$50	T3 Confused	0.36	P.Search	**Q.Rephrase**
4	No results for orig. query	T3 Confused	0.37	**P.Search**	Q.Rephrase
5	6 results for new query	T5 Optimistic	0.41	P.Compare	P.Compare
6	Item #3: $38, ★4.2	T4 Approving	0.58	Purchase	Purchase
Episode outcome				**Failure**	**Success**

Figure 6 shows the full emotion trajectory of this episode: encoder confidence, selected template, and shift magnitude δ_t. The transition point at step 4 (δ=0.42 $>$ $\bar{\delta} + \sigma_\delta$) is also the trigger for evolution in Case B.

Case B: Emotion-Driven Skill Evolution *WebShop, Qwen3-8B, Round 2*

After round 1, QUERYREPHRASE succeeds in only 38% of episodes ($<$ η=40%) and is flagged for evolution. Transition diagnostics at step 4 (δ=0.42) and step 6 (δ=0.39)

identify a recurring Confused→Confused pattern. The verbalized summary Δ_i: *"The agent repeatedly enters Confused states during rephrasing with no exit criterion; the SOP lacks a budget and escalation path."* The evolved SOP directly addresses the diagnosed failure.

Original SOP	Evolved SOP (Round 2)
When results don't match, try synonyms or broader terms and re-search. Continue until a match is found or the task is abandoned.	**(1)** Identify the specific failing keyword. **(2)** Try up to **3 alternative queries**: synonyms → broaden noun → drop most restrictive attribute. **(3)** If all 3 fail, **exit to ProductSearch** with core noun + price range only. Do not rephrase >3 times; escalate promptly to avoid confusion loops.

Triggers: δ=0.42 at step 4 and δ=0.39 at step 6 (Confused → Confused). Root cause: no rephrasing budget or exit criterion.

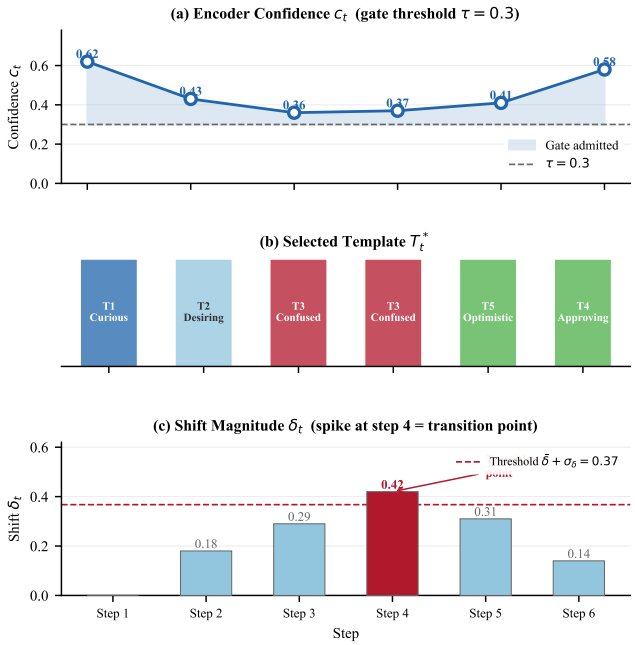

Figure 6: Emotion trajectory from Case A (WebShop, Qwen3-8B). (a) Encoder confidence c_t; gate threshold τ=0.3 shown dashed. (b) Selected template T_t^*, color-coded by state. (c) Shift magnitude δ_t; transition threshold $\bar{\delta} + \sigma_\delta$ dashed. Step 4 (δ=0.42) is the transition point that triggers QUERYREPHRASE and informs the evolution in Case B.

Case C: Pre-Action Emotion Signal Prevents Failure *ALFWorld Heat, Qwen3-8B*

Heat tasks improve most dramatically (9.6% → 56.9%). The task: heat a mug and place it on the counter.

Baseline failure. The agent navigates to the microwave and issues `heat mug`. Feedback arrives: *"Action failed: microwave is closed."* The failure signal is available only *after* the incorrect action.

Emotion2Skill. When the agent approaches the closed microwave, the encoder detects T9 Nervous (c_t=0.34 > τ), reflecting internal apprehension about unverified preconditions, *before* any action is taken. The emotion-augmented prompt routes to an examine → open → heat sub-sequence; the task succeeds.

After round-1 evolution. The transition diagnostic (T9 Nervous at the microwave approach step) is used to localize the SOP gap. The evolved HEAT OBJECT SOP gains the precondition check: *"Before heating, verify the appliance is open; if closed, open it first."* This single addition, directly derived from the T9 transition, accounts for a large fraction of the +47.3 pp gain on Heat tasks.

F Additional Results

F.1 Evolution Round-by-Round

Table 12 compares emotion-guided evolution against outcome-only evolution across the three rounds.

Method	Round 1	Round 2	Round 3
Evo-Outcome (no diagnostics)	26.8	27.5	28.1
Evo-Emotion (ES)	27.2	28.9	**29.7**
Δ	+0.4	+1.4	+1.6

Table 12: WebShop Succ. (%) across evolution rounds (Qwen3-8B). Emotion diagnostics yield compounding gains; the gap widens to +1.6 pp by round 3 as more transition evidence accumulates.

F.2 Per-Task Emotion Patterns on ALFWorld

Table 13 shows the most frequently activated template per ALFWorld task type on correctly-solved episodes. Procedure-heavy tasks (Heat, PickTwo) activate frustration/confusion, consistent with their multi-step error-recovery demands.

Task	Top Template	Freq.
Pick	T1 Curious	42%
Look	T4 Approving	38%
Clean	T3 Confused	35%
Heat	T7 Frustrated	41%
Cool	T10 Realizing	33%
PickTwo	T3 Confused	39%

Table 13: Most frequent emotion template per ALFWorld task type (Qwen3-8B, correctly-solved episodes only).

F.3 Confidence Score Distribution

Figure 7 shows the distribution of encoder confidence scores c_t across all WebShop test steps. The distribution is right-skewed, with the bulk of steps concentrated in the range $c_t \in [0.30, 0.60]$ and a sparse high-confidence tail above 0.70. A substantial minority of steps (28%) fall below τ=0.3 and trigger the text-only fallback, reflecting genuine uncertainty at ambiguous or transitional states. The remaining 72% are admitted by the gate and benefit from emotion-augmented skill selection.

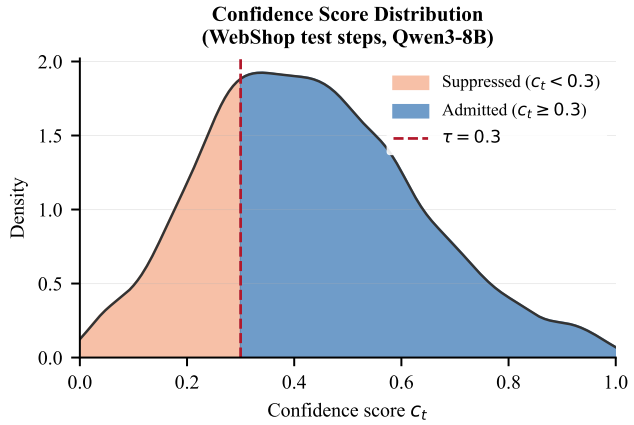

Figure 7: Confidence score distribution (WebShop, Qwen3-8B). Mass concentrated in $c_t \in [0.30, 0.60]$ with a sparse high tail; 72% of steps are gate-admitted (blue), 28% suppressed (orange). Gate threshold τ=0.3 shown as dashed line.

G Limitations and Broader Impact

Limitations. White-box residual-stream access is required, limiting direct application to API-served LLMs; distilling routing signals to black-box models is a natural extension. The warm-up phase collects ∼500 episodes (<10 min); few-shot encoder initialization could reduce this. Emotion-guided routing does not uniformly dominate all task types: on ALFWorld Cool tasks, EMOTION2SKILL is outperformed by MASA on Qwen3-8B, suggesting that tasks with highly stereotyped action sequences may benefit less from emotion-based rerouting and could benefit from adaptive per-task thresholding as future work. Instruction-tuned variants with modified hidden-state geometry may require re-extraction (Qwen3-8B-Instruct GoEmotions accuracy: 28.1% vs. 37.2% on the base model). Extension to multi-agent coordination is left open.

Broader Impact. Making LLM internal states actionable improves interpretability and debuggability of agent systems. In high-stakes domains (healthcare, finance), the confidence-gating mechanism provides a built-in safety fallback when the emotion signal is uncertain. Access to internal model states could theoretically be misused for surveillance; responsible deployment requires appropriate access controls. On balance, we believe the transparency and adaptive-control benefits outweigh the risks.

H Notation Summary

Table 14 provides a consolidated reference for all mathematical symbols used in the paper, grouped by subsystem.

Symbol	Definition
Agent and task	
$\mathcal{M}$	LLM agent backbone (Qwen3-8B or Qwen3-14B, non-thinking mode)
$\mathcal{S} = \{s_1, \ldots, s_M\}$	Skill library of M skills; D_i: natural-language SOP for skill s_i
x_t	External textual context at step t (task instruction, history, observation)
s_t^*	Skill selected at step t
$r_{\text{ep}} \in \{0, 1\}$	Episode outcome (1 = success)
LLM internals	
$\mathbf{h}_t^{(\ell)} \in \mathbb{R}^d$	Residual-stream activation at layer ℓ, token position t; d: hidden dim
L^*	Optimal extraction layer (selected by GoEmotions validation accuracy)
$\bar{\mathbf{h}}^{(\ell)}$	Mean-pooled per-story activation at layer ℓ (tokens $t \geq 50$)
Emotion direction extraction (offline)	
$K = 27$	Number of GoEmotions emotion concepts
$N = 100$	Stories generated per emotion concept
$\mu_k^{(\ell)}$	Within-class mean activation for concept k at layer ℓ
$\bar{\mu}^{(\ell)}$	Global mean over all KN story activations at layer ℓ
$\mathbf{v}_k^{(\ell)} \in \mathbb{R}^d$	Contrastive emotion direction: $\mu_k^{(\ell)} - \bar{\mu}^{(\ell)}$ (Eq. 1)
$\Pi^{\perp}$	PCA denoising projector (removes top neutral-activation components)
$\hat{\mathbf{v}}_k^{(\ell)}$	Denoised direction: $\Pi^{\perp}\mathbf{v}_k^{(\ell)}$
$W_e \in \mathbb{R}^{K \times d}$	Emotion extractor matrix; rows $= \hat{\mathbf{v}}_k^{(L^*)}$
Online emotion state	
$\mathbf{e}_t \in \mathbb{R}^K$	ℓ_2-normalized emotion state at step t: $W_e\mathbf{h}_T^{(L^*)} / \lVert W_e\mathbf{h}_T^{(L^*)} \rVert_2$ (Eq. 2)
f_θ	Emotion encoder: 3-layer MLP (27→64→128→128, ReLU, <27K params)
$\mathbf{r}_t \in \mathbb{R}^{128}$	Encoded representation: $f_\theta(\mathbf{e}_t)$
Template selection and confidence gating	
$C = 12$	Number of emotion-state templates
$\mathcal{T} = \{T_1, \ldots, T_C\}$	Template bank (task-agnostic; Table 11)
$\mathbf{q}_j \in \mathbb{R}^{128}$	Learnable prototype for template T_j
T_t^*	Selected template: $\arg\max_j \cos(\mathbf{r}_t, \mathbf{q}_j)$ (Eq. 3)
$c_t \in [0, 1]$	Confidence score: $\sigma(\mathbf{w}_c^{\top}\mathbf{r}_t + b_c)$ (Eq. 4)
τ	Confidence gate threshold (default 0.3, tuned on WebShop validation)
$\boldsymbol{\phi}_t = (T_t^*, c_t)$	Composite emotion summary injected into P_t
P_t	Augmented prompt at step t (Eq. 5); reduces to text-only when $c_t < \tau$
Encoder training losses	
$\mathcal{A}^+(i)$	Positive set for anchor i: same skill & successful outcome
$\mathcal{L}_{\text{ctr}}$	Supervised-contrastive loss (Eq. 6); temperature κ=0.07
$\mathcal{L}_{\text{cls}}$	Template-classification loss (Eq. 7); temperature κ'=0.1
λ	Loss weight: $\mathcal{L} = \mathcal{L}_{\text{ctr}} + \lambda\mathcal{L}_{\text{cls}}$, default λ=0.5
Skill evolution	
$\mathcal{E} = (\mathbf{e}_1, \ldots, \mathbf{e}_T)$	Episode emotion trajectory
$\delta_t = 1 - \mathbf{e}_t^{\top}\mathbf{e}_{t-1}$	Step-to-step cosine distance (Eq. 8)
$\bar{\delta}$, σ_δ	Episode mean and std of δ_t values
$\mathcal{P}$	Transition-point set: $\{t \mid \delta_t > \bar{\delta} + \sigma_\delta\}$ (Eq. 9)
$\mathcal{P}_i$	Skill-specific transitions: $\{t \in \mathcal{P} \mid s_t^* = s_i\}$
w	Diagnostic window half-width (default w=1; 3-step context)
$\mathbf{d}_t$	Diagnostic context: $(x_{t-w:t+w}, s^*_{t-w:t+w}, T^*_{t-w:t+w}, \delta_{t-w:t+w})$ (Eq. 10)
Δ_i	Verbalized transition summary for skill s_i
$P_{\text{evo}}^{(i)}$	Evolution prompt for skill s_i (Eq. 11)
D_i'	Revised SOP generated by the LLM rewriter (Eq. 12)
$\mathcal{U}^{(r)}$	Underperforming skills in round r (success rate $< \eta$)
η	Performance threshold for flagging skills (default 0.4)
R	Number of evolution rounds (default 3)

Table 14: Complete notation reference. Symbols are grouped by the pipeline stage in which they first appear. Standard notation ($\mathcal{M}$, D_i, x_t) is also defined inline where first used in the main text.